



Published in final edited form as:

Xenobiotica. 2015 ; 45(8): 711–721. doi:10.3109/00498254.2015.1016475.

Metabolic disposition of the anti-cancer agent [¹⁴C]laromustine in male rats

Ala F. Nassar^{1,2}, Adam Wisnewski¹, and Ivan King³

¹Department of Internal Medicine, School of Medicine, Yale University, New Haven, CT, USA

²Department of Chemistry, University of Connecticut, Storrs, CT, USA

³Metastagen, Inc., Wilmington, DE, USA

Abstract

1. Laromustine (VNP40101M, also known as Cloretazine) is a novel sulfonylhydrazine alkylating (anticancer) agent. This article describes the use of quantitative whole-body autoradiography (QWBA) and mass balance to study the tissue distribution, the excretion mass balance and pharmacokinetics after intravenous administration of [¹⁴C]VNP40101M to rats. A single 10 mg/kg IV bolus dose of [¹⁴C]VNP40101M was given to rats.
2. The recovery of radioactivity from the Group 1 animals over a 7-day period was an average of 92.1% of the administered dose, which was accounted for in the excreta and carcass. Most of the radioactivity was eliminated within 48 h via urine (48%), with less excreted in feces (5%) and expired air accounted for (11%). The plasma half-life of [¹⁴C]laromustine was approximately 62 min and the peak plasma concentration (C_{max}) averaged 8.3 µg/mL
3. The QWBA study indicated that the drug-derived radioactivity was widely distributed to tissues through 7 days post-dose after a single 10 mg/kg IV bolus dose of [¹⁴C]VNP40101M to male pigmented Long–Evans rats. The maximum concentrations were observed at 0.5 or 1 h post-dose for majority tissues (28 of 42). The highest concentrations of radioactivity were found in the small intestine contents at 0.5 h (112.137 µg equiv/g), urinary bladder contents at 3 h (89.636 µg equiv/g) and probably reflect excretion of drug and metabolites. The highest concentrations in specific organs were found in the renal cortex at 1 h (28.582 µg equiv/g), small intestine at 3 h (16.946 µg equiv/g), Harderian gland at 3 h (12.332 µg equiv/g) and pancreas at 3 h (12.635 µg equiv/g). Concentrations in the cerebrum (1.978 µg equiv/g), cerebellum (2.109 µg equiv/g), medulla (1.797 µg equiv/g) and spinal cord (1.510 µg equiv/g) were maximal at 0.5 h post-dose and persisted for 7 days.

Address for correspondence: Dr. Ala F. Nassar, PhD, Department of Internal Medicine, Yale University, New Haven, CT, USA. ala.nassar@yale.edu.

Declaration of interest

The authors report no conflicts of interest. The authors alone are responsible for the content and writing of this article.

4. The predicted total body and target organ exposures for humans given a single 100 μ Ci IV dose of [14 C]VNP40101M were well within the medical guidelines for maximum radioactivity exposures in human subjects.

Keywords

Anti-cancer agent; mass balance; quantitative whole-body autoradiography

Introduction

Laromustine [VNP40101M, 1,2-bis(methylsulfonyl)-1-(2-chloroethyl)-2-(methylamino)carbonylhydrazine] is an active member of a relatively new class of sulfonylhydrazine prodrugs under development as antineoplastic alkylating agents (Baumann et al., 2005; Penketh et al., 2004). The chemical structure of laromustine is shown in Figure 1. Laromustine generates two distinct types of reactive intermediates: 90CE and methylisocyanate. 90CE and other hard chloroethylating (DNA-reactive) species alkylate DNA at the O⁶-position of guanine residues that progress to G-C interstrand cross-links (Penketh et al., 2000, 2004). Methylisocyanate, a soft electrophilic carbamoylating agent, binds preferentially and stoichiometrically to sulfhydryl groups and inhibits a number of enzymes, including O⁶-alkylguanine-DNA-alkyltransferase (AGT), a DNA repair enzyme. The release of methylisocyanate and its inhibition of DNA repair by AGT is thought to augment the antineoplastic effect of 90CE and related chloroethylating species. This process probably accounts for the considerably greater antineoplastic activity of laromustine relative to that of other sulfonylhydrazine alkylating agents, many of which generate 90CE like laromustine, but in contrast to laromustine do not generate methylisocyanate (Baumann et al., 2005). Laromustine displays anticancer activity against a broad spectrum of transplanted tumors (Finch et al., 2001) and exhibited antileukemic activity in initial clinical trials (Giles et al., 2004).

Mass balance studies using radiolabeling can facilitate the quantification of the drug and drug-related substances in blood, plasma, urine and feces collected from the study subjects. Information about the total fate of drug-related material and routes of excretion can be obtained from mass balance studies (Park et al., 1997; Schadt et al., 2012). QWBA studies provide the tissue distribution and pharmacokinetics data required for new drug registration and for predicting human exposure to radioactivity during clinical radiolabeled mass balance studies (Gifford et al., 2008; Wang et al., 2011). Both QWBA and mass balance studies are required for regulatory filings of a new drug entity and for projecting tissue dosimetry in human mass balance studies (Scicinski et al., 2012).

Recently, we reported an *in vitro* evaluation of the victim and perpetrator potential of the anti-cancer agent laromustine (Nassar et al., 2009). In addition, the *in vitro* metabolite profiling and mass balance of [14 C]VNP40101M in rat, dog, monkey and human liver microsomes was reported (Nassar et al., 2010a,b,c). The *in vitro* studies found that VNP40101M and VNP4090CE undergo activation in human liver microsomes. Phase 1 metabolism of laromustine was reported recently and showed that laromustine undergoes rearrangement, dehalogenation and hydrolysis at physiological pH to form active moieties

(Nassar et al., 2010a,b,c, 2011). This article describes the investigation of tissue sections and mass balance of rats after a single 10 mg/kg IV bolus dose of [¹⁴C]VNP40101M.

Materials and methods

[¹⁴C]Laromustine (labeled in the ethane side chain, see Figure 1, asterisks indicate site of ¹⁴C-label). The radiolabeled test article was stored in a -20 °C freezer protected from light, and the non-radiolabeled material was stored at 2–8 °C. As determined by Moravek Biochemicals, Inc. (Brea, CA), the specific activity was 57.3 mCi/mmol. Prior to use, the radiochemical purity of [¹⁴C]VNP40101M was confirmed using an HPLC method. All chemicals and reagents used were analytical grade, and the chromatographic solvents used were HPLC grade. Some of the equipment used for this study included liquid scintillation counter (Packard Bioscience Company model TR-2900), sample oxidizer (Packard Bioscience Company model 307) and stomach circulator (Seward model 400).

Mass balance

Dose administration

This study was performed using a total of 12 male Sprague–Dawley rats (not including replacement animals and blood donors): 4 assigned to Group 1 (excretion mass balance), 4 assigned to Group 2 (expired air collection) and 4 assigned to Group 3 (pharmacokinetics). Animals were not fasted overnight prior to [¹⁴C]VNP40101M dose administration. The volume of the dose solution administered to each rat was determined based upon the pre-dose body weight of each animal obtained the morning of dosing. Each animal in Group 1, 2 and 3 received a single intravenous bolus dose of [¹⁴C]VNP40101M at a target dose of 10 mg/kg. The IV dose volume was 2 mL/kg. The dose was administered through a femoral vein cannula. The dose contained a combination of non-radiolabeled VNP40101M and [¹⁴C]VNP40101M to achieve the target doses as shown below.

Study groups and target doses.

Group number	No./sex of animals	Dose route	Target dose concentration (mg/mL)	Target dose volume (mL/kg)	Target dose (mg/kg)	Target radioactivity dose (μCi/kg)
1 (FVC)	4/M	IV	5	2	10	100
2 (FVC)	4/M	IV	5	2	10	100
3 (FVC/JVC)	4/M	IV	5	2	10	100

Test animals

Male Sprague–Dawley rats used in this study were 7 weeks old on day of dosing and were obtained from Hilltop Laboratories (Scottsdale, PA). Animals were acclimated in the test facility at least 2 days before study initiation. Before being placed in the study, each animal was weighed, assigned a permanent identification number, and identified with a tail mark. All the animals were not fasted and weighed between 255 and 344 g at the time of dosing.

Formulations

Dosing formulations were freshly prepared on the day of dosing and assayed for radioactivity concentration on each day of dosing. The IV dosing formulation was prepared by diluting a stock solution containing 10 mg/mL VNP40101M in 30% ethyl alcohol, 70% polyethylene glycol 300, 6 mg/mL citric acid, with [^{14}C]VNP40101M and 5% dextrose in water (D₅W). The administered formulation thus contained 5 mg/mL VNP40101M, 15% ethanol and 35% polyethylene glycol 300 in D₅W. The solution was vortexed to achieve homogeneity. The dose solution was stirred continuously using a magnetic stirrer throughout the dose administration procedure.

Sample collections

Animals study design and dosing regimen

Group 1: Feces, urine, cage rinses, cage washes, cage wipes and carcasses: Group 1 rats were housed in plastic (Nalgene[®]) metabolism cages. Urine samples were collected into labeled polypropylene containers maintained on dry ice at pre-dose and at post-dose intervals of 0–4, 4–8, 8–24 and at 24 h intervals up to 168 h. Feces samples were collected into labeled polypropylene containers maintained on dry ice at pre-dose, 0–24 h and at 24 h post-dose intervals up to 168 h. A post-dose cage rinse was performed for each metabolism cage at each 24 h interval after urine and feces collections, up to 144 h post-dose. Cage rinses were performed with approximately 30 mL of a mixture of reagent alcohol/ deionized water (50:50). After the last excreta collection at 168 h post-dose, each cage was washed with approximately 90 mL of RadiacWash (100%) and wiped down with gauze pads (cage wipe). At 168 h post-dose, the body weight of each animal was measured and then each animal was euthanized in a CO₂ chamber. Each carcass was stored in a labeled plastic bag and retained for radioanalysis. The weight of each sample (i.e. urine, feces, cage residues and carcasses) was recorded in the study records.

Group 2: expired air: Group 2 rats were housed in glass metabolism cages required for the collection of expired air. The circulating air exiting the cage was passed through absorption columns where the expired $^{14}\text{CO}_2$ gas was trapped in a solution of Carbo-Sorb[®]. The $^{14}\text{CO}_2$ scrubber liquids were collected from the system during pre-dose, 0–24 and 24–48 h post-dose.

Group 3: blood for plasma pharmacokinetics: Group 3 rats were housed in plastic metabolism cages. Blood samples were collected from Group 3 animals for characterizing the pharmacokinetics of plasma radioactivity. The blood samples were collected at pre-dose, 0.083, 0.25, 0.50, 1, 2, 4, 7, 10, 24 and 48 h post-dose. The blood samples for each rat (~0.8 mL) were collected from the jugular vein cannula into tubes containing sodium heparin as an anticoagulant and 0.02 mL of 2 M citric acid as a stabilizing agent. Samples were centrifuged within 1h of collection at 3000 rpm for 10 min at 4°C and plasma was harvested, snap frozen and stored at – 70 °C. After blood withdrawal, approximately 0.8 mL of fresh blood from a donor rat was transfused back into each rat. Blood donor animals were healthy naive Sprague–Dawley rats.

Sample preparation and radioanalytical methods

All samples directly counted by LSC (plasma, urine, cage rinse, cage wash, extracts of cage wipes and solubilized carcasses) were analyzed using Ultima Gold scintillation cocktail (Packard, Groningen, The Netherlands). All samples were counted using a Model 2900TR liquid scintillation analyzer (Packard, Groningen, The Netherlands) and counting was for at least 5 min or 100 000 counts. The LSC data in counts per minute (cpm) were automatically corrected for counting efficiency using an external standard and an instrument-stored quench curve generated from sealed quenched standards to obtain disintegrations per minutes (dpm). The LSC data were corrected for background by subtracting the dpm value measured from the analysis of a blank sample. Dosing solution aliquots and feces homogenates were analyzed in triplicate. Urine, plasma, expired air and cage residues (i.e. rinse, wash and wipe) were analyzed in duplicate. If results for duplicate samples (calculated as ^{14}C dpm/g sample) differed by more than 10% from the mean value, the sample was re-homogenized (where appropriate) and reanalyzed. If results for triplicate sample replicates had a %CV greater than 10%, the sample was re-homogenized (where appropriate) and reanalyzed. This specification was met for all sample aliquots that had radioactivity greater than 500 dpm.

Analysis of urine (Group 1)

Prior to analysis and immediately after removal from the storage freezer, 2 M citric acid at a volume of 2.5% of the sample weight was added to each urine specimen, and then the specimens were thawed. Each sample was brought to room temperature, mixed thoroughly and duplicate aliquots (target 0.5 mL) were transferred to labeled scintillation vials. After adding 10 mL of Ultima Gold scintillation cocktail to each sample and mixing, the samples were analyzed for radioactivity.

Analysis of feces (Group 1)

Feces samples were thawed and brought to room temperature, mixed with 0.1 M citric acid (ca. 2–3 times the feces weight and enough to create a slurry), and the total homogenate weight was recorded. All the samples were homogenized using a Stomacher 400 Circulator. Triplicate weighed aliquots (ca. 0.5 g) of each homogenate were added to Combusto Cones[®] with Combusto Pads[®] and placed in labeled scintillation vials. Fecal samples were combusted in a Model 307 Sample Oxidizer (Packard Instrument Co., Downers Grove, IL) and the resulting $^{14}\text{CO}_2$ was trapped in CarboSorb. Perma-Fluor scintillation cocktail (Packard) was added and the radioactivity content quantitated by LSC.

Analysis of cage wash, cage rinse and cage wipe specimens (Group 1)

Cage wash and cage rinse samples were thawed, brought to room temperature. Duplicate aliquots (0.5 mL) of cage wash and cage rinse samples were transferred to labeled scintillation vials and Ultima Gold scintillation cocktail (10 mL) was added. Samples were then analyzed for radioactivity.

Cage wipes from each cage were thawed, transferred to a labeled polypropylene container and soaked overnight at room temperature in 50% methanol:50% distilled water to extract [^{14}C]-radioactivity. Duplicate sample aliquots (0.5 mL) were transferred to labeled

scintillation vials and Ultima Gold scintillation cocktail (10 mL) was added. Samples were then analyzed for radioactivity.

Analysis of carcasses (Group 1)

Carcasses were solubilized in 6N KOH by stirring at room temperature until particulate matter was no longer present. Once homogenized, triplicate weighed aliquots (ca. 0.5 g each) were removed, bleached using hydrogen peroxide and analyzed for radioactivity.

Analysis of expired air (Group 2)

The Carbo-Sorb[®] trapping solution (expired air samples) was allowed to approach room temperature, mixed thoroughly and duplicate aliquots (0.5 mL) of individual samples were transferred to labeled scintillation vials. Hionic Fluor scintillation cocktail (10 mL) was added and samples were then analyzed for radioactivity using LSC.

Analysis of plasma samples (Group 3)

Plasma samples were thawed and brought to room temperature, mixed thoroughly and duplicate aliquots (0.05 mL) were transferred to labeled scintillation vials. Ultima Gold scintillation cocktail (10 mL) was added, and the samples were mixed and analyzed for radioactivity.

Calculations used for sample analysis

Samples not homogenized:

$$\text{Sample dpm/g (or/mL)} = \text{Sample aliquot dpm} / \text{Sample aliquot weight (or volume)}$$

Samples homogenized:

$$\text{Homogenate dpm/g (or/mL)} = \text{Homogenate aliquot dpm} / \text{Homogenate aliquot weight (or volume)}$$

$$\text{Sample total dpm} = \text{Homogenate dpm/g (or/mL)} \times \text{Total homogenate weight (or volume)}$$

$$\text{Sample dpm/g (or/mL)} = \text{Sample total dpm} / \text{Sample total weight (or volume)}$$

All samples

LSC LLOQ = 2 × cpm of background vial with background subtraction (any value lower than LLOQ were set to zero for calculation)

$$\text{Coefficient of variation (\%CV)} = \frac{\text{Standard deviation (SD)}}{\text{Mean}} \times 100$$

$$\text{Percent of mean} = 100 - \frac{\mu\text{Ci per gram (or per mL)}}{\text{Mean } (\mu\text{Ci per gram (or per mL)})} \times 100$$

$$\mu\text{Ci/g (or/mL)} = \frac{\text{Sample dpm/gram (or per mL)}}{2.22 \times 10^6 \text{ dpm per } \mu\text{Ci}}$$

$$\mu\text{g equivalents/g (or/mL)} = \frac{\mu\text{Ci per gram (or per mL)}}{\text{Specific activity dosed}}$$

$$\text{Total } \mu\text{Ci in sample} = \text{Mean } \mu\text{Ci/g(or/mL)} \times \text{Total sample weight}$$

$$\text{Percent recovery of radioactivity} = \frac{\text{Total } \mu\text{Ci in sample}}{\text{Total } \mu\text{Ci dosed}} \times 100$$

Data analysis

The following criteria were used to determine the acceptance or re-analysis of liquid scintillation counting (LSC) results: excluding plasma samples, if the LSC results for duplicate samples (calculated as dpm/g sample) differed by more than 10% from the mean value, the remaining sample was re-aliquoted and reanalyzed. The initial LSC results for duplicate plasma aliquots were reported as determined since there was insufficient volume for sample reanalysis. If LSC results for triplicate samples had a CV >10% and an average radioactivity greater than 500 dpm, the remaining sample was re-homogenized and reanalyzed. Data tables were compiled with the mean and standard deviation calculated using Excel. The data presented in the summary tables reflect the data recorded in the study records and the data presented in the report text have been rounded appropriately to summarize results. Non-compartmental pharmacokinetic parameters were calculated for plasma concentrations using WinNonlin™ (Pharsight Corporation, Sunnyvale, CA). The λ_z was obtained, where possible, by linear regression of the terminal elimination phase of a log-linear plot of plasma concentration-time data. The observed maximum plasma concentration (C_{\max}) was determined directly from the concentration-time profile. The area under the plasma concentration-time curve from time 0 to the last quantifiable plasma concentration (AUC_{0-t} ; AUC_{0-t} was equivalent to $AUC_{0-48 \text{ h}}$ in this study) and the area under the plasma concentration-time curve from time 0 to infinity [$AUC_{(0-\infty)}$] were determined by the linear trapezoidal rule.

Whole-body autoradiography

Dose solution and analysis

Prior to dosing, the concentration and homogeneity of each formulation were checked using LSC. Triplicate pre-dose and post-dose aliquots (0.1 mL from each of top, middle and bottom of vial) of the dose solution were taken and diluted to 10 mL with ethanol. Aliquots of the diluted dose solutions were analyzed for 10 min by LSC. The mean pre-dose radioactivity concentration was used in calculating the amount of radioactivity administered to each animal. The mean concentration of radioactivity was 38.1 $\mu\text{Ci/g}$ (pre-dose assay). The radiochemical purity of [^{14}C]VNP40101M in the dosing formulation was examined by

radio-HPLC in both pre-dose and post-dose aliquots. The stability of [^{14}C]VNP40101M in the dose solution was determined by analyzing pre-dose and post-dose aliquots by the radio-HPLC method, and the test article was considered to be stable under the conditions of dose formulation preparation and through the completion of dose administration.

Animal experimentation

Eleven male pigmented Long–Evans rats, approximately 8 weeks old, with a body weight range of 240.2–278.1 g, with cannulated femoral veins, were used for this study. The Long–Evans rats were supplied by Hilltop Lab Animals, Inc. (Scottsdale, PA). All the rats were maintained on Certified Rodent Diet[®] #5002 (PMI Nutrition International, Richmond, IN), and filtered water from domestic supply (Artesian Water, Inc., Newark, DE) provided *ad libitum*. The rats were not fasted prior to dosing. Animals were kept under controlled environmental conditions, where the temperature and humidity range settings were set to maintain 65–75°F and 20–70%, respectively. Animal rooms were set for at least 10 air exchanges per hour (h) and the room lighting cycle on a 12 h light/dark cycle. Each animal was randomized and given a unique study-specific identification number and identified by tail-marking. Rats were housed in shoebox cages with wire mesh bottoms. Their body weights were determined prior to dosing. Each animal received a single IV dose at a nominal dose of 10 mg/kg via a femoral vein cannula, which was based on pre-dose body weight. The doses administered were determined by weighing the syringes before and after administration. After dosing, all the rats were returned to their cages. Cage-side observations were performed three times post-dose on the day of dosing and at least daily for the remainder of the study, as appropriate, and any observations were recorded. One pigmented rat per time point was scheduled for euthanasia at 0.5, 1, 3, 6, 8 and 24 h, and 2, 3, 4, 5 and 7 days post-dose. Animals scheduled for euthanasia were deeply anesthetized with isoflurane, euthanized and frozen by submersion in a hexane/dry ice bath. All carcasses were stored at approximately –20 °C prior to preparation for whole-body autoradiography.

The frozen carcasses were embedded in a 2% carboxymethylcellulose matrix and mounted on a microtome stage (Leica CM3600 Cryomacrocut, Nussloch, Germany) maintained at approximately –20 °C. Three quality control standards (QC), which were 2% carboxymethylcellulose fortified with [^{14}C]glucose at one concentration (0.057 $\mu\text{Ci/g}$), were placed into the frozen blocks prior to sectioning, and were used for section thickness quality control as per QPS SOP #WBA-003. Sections approximately 40 μm thick were taken in the sagittal plane, and captured on adhesive tape (Scotch Tape No. 8210, 3M Ltd., St. Paul, MN). Appropriate sections selected at various levels of interest in the block were collected to encompass the following tissues, organs and biological fluids, where possible: adipose (brown and white), adrenal gland, bile (in duct), blood, brain (cerebrum, cerebellum, medulla), bone, bone marrow, cecum (and contents), epididymis, eye (uveal tract and lens), Harderian gland, heart, kidney (renal cortex and medulla), large intestine (and contents), liver, lung, lymph node, pancreas, pituitary gland, prostate gland, salivary gland, seminal vesicles, skeletal muscle, skin, stomach (gastric mucosa and contents), small intestine (and contents), spleen, spinal cord, testis, thymus, thyroid and urinary bladder (and contents).

Sections were allowed to dry by sublimation in the cryomicrotome at $-20\text{ }^{\circ}\text{C}$ for at least 48 h after cutting. A set of sections were mounted on a cardboard backing, covered with a thin plastic wrap, and exposed along with calibration standards of ^{14}C -blood (0.0008, 0.0009, 0.0012, 0.0017, 0.0021, 0.0034, 0.0065, 0.0125, 0.0267, 0.0516, 0.1028, 0.2081, 0.7680, 3.5737 and 8.1770 $\mu\text{Ci/g}$) to ^{14}C -sensitive phosphor imaging plates (Fuji Biomedical, Stamford, CT). The image plates and sections were placed in light-tight exposure cassettes for a 4-day exposure at room temperature. The image plates were scanned using the Typhoon 9410[®] image acquisition system (GE/Molecular Dynamics, Sunnyvale, CA) and the resultant images stored by a dedicated QPS computer server. Quantification was performed by image densitometry using MCID image analysis software (v. 6.0 or higher, GE/Imaging Research Inc., St. Catherines, Ontario, Canada) and a standard curve constructed from the integrated response (MDC/ mm^2) and the nominal concentrations of the ^{14}C -blood standards. The concentrations of radioactivity were expressed as the μg equivalents of VNP40101M per gram sample ($\mu\text{g equiv/g}$).

Results and discussion

Mass balance

All animals appeared to be healthy at the start of the study and animals from Group 1 and Group 2 completed the study without incident. Group 3 rats (Rats 9, 10, 11 and 12) exhibited labored breathing and died within a few minutes after blood transfusion following the 7 h blood sample collection. After a complete investigation by the attending veterinarian, the cause of death was attributed to acute pulmonary distress precipitated by the infusion of particulates present in the donor blood. The deaths were not attributed to VNP40101M. A replacement cohort of Group 3 animals were dosed 1 week later (Rats 9A, 10A, 11A and 12A) and no adverse events were noted during the course of the study.

As shown in Figure 2, most of the dose was excreted in the urine, with $51.4 \pm 1.0\%$ recovered within 168 h post-dose. The majority (46.7%) of this excretion occurred within 24 h. Fecal excretion of the IV dose, $5.6 \pm 0.6\%$, suggests biliary excretion may be a minor route for the elimination of VNP40101M and metabolites. A significant portion of the dose ($21.7 \pm 6.9\%$) was retained in the carcass 168 h post-dose. This may not be unexpected given the mechanism of action for the molecule. The mean total recovery of radioactivity in urine, feces, cage rinses, cage washes, cage wipes and carcass was $81.1 \pm 5.6\%$. The total recovery of volatile radioactivity was $11.0 \pm 1.2\%$, with 9.6% recovered within the first 24 h. When these results were added to the recovery of radioactivity from the Group 1 animals, an average of 92.1% of the administered dose was accounted for in the excreta and carcass.

Individual and mean plasma radioactivity concentrations for Group 3 rats are given in Table 1 and are plotted in Figure 3. In Group 3 rats, the mean maximum plasma radioactivity concentration ($8.352 \pm 0.805\ \mu\text{g equivalents/mL}$) was observed at 0.083 h, the first sample collection time. Total radioactivity in plasma declined with a mean terminal half-life of $61.8 \pm 11.3\text{ h}$, with a mean radioactivity of $1.408 \pm 0.115\ \mu\text{g equivalents/mL}$ detected in plasma at 48 h post-dose. These pharmacokinetic estimates, representing both parent and metabolites, must be interpreted cautiously because sampling was only carried out to 48 h post-dose.

Quantitative whole-body autoradiography

There were no remarkable observations throughout the study for all the rats. Whole-body autoradiograms show the patterns of radioactivity distribution in tissues. Figure 4 is a representative QWBA profile of the radioactivity distribution in a male pigmented rat at 0.5 h Post-dose following a single IV administration of [¹⁴C]VNP40101M at a target dose of 10 mg/kg. The concentrations of drug-derived radioactivity in the tissues of rats following IV bolus administration of [¹⁴C]VNP40101M are summarized in Table 2. Forty-two areas representing highly and poorly perfused organs, important target organs like liver, lung and brain and excreta (urinary bladder contents, bile and cecal contents) were sampled. Drug-derived radioactivity was widely distributed to tissues. Maximum concentrations were observed 0.5 or 1 h post-dose for most tissues (28 of 42). The highest concentrations of radioactivity were found in the small intestine contents at 0.5 h (112.137 µg equiv/g), and urinary bladder contents at 3 h (89.636 µg equiv/g), which probably reflect excretion of drug and metabolites. The highest concentrations in specific organs were found in the renal cortex at 1 h (28.582 µg equiv/g), small intestine at 3 h (16.946 µg equiv/g), Harderian gland at 3 h (12.332 µg equiv/g) and pancreas at 3 h (12.635 µg equiv/g). Concentrations in the cerebrum, cerebellum, medulla and spinal cord were maximal at 0.5 h post-dose and persisted for 7 days. The radioactivity was mostly eliminated over 7 days, which suggested the potential for distribution into tissues. The calculated half-lives for the elimination of total radioactivity from tissues ranged from 51 h for the Harderian gland to 262 h for white adipose tissue. These values must be interpreted cautiously because only one animal was sampled at each time point and the inter-animal variability is unknown. Tissue concentrations 7 days post-dose were generally up to 4-fold the LLOQ (0.108 µg equiv/g); some of them (19 of 42 samples) were BQL.

Human dosimetry predictions

The individual predicted human tissue exposures to radioactivity after a 100 µCi, IV dose of [¹⁴C]VNP40101M were summarized and can be found in Table 2. The predicted tissue exposure in humans given a single 100 µCi IV dose of [¹⁴C] VNP40101M is shown in Table 3. The predicted exposure was less than 0.4% of the 3–5 rem limits specified by the Code of Federal Regulations (21 CFR: part 361.1, section b, 3i). Consistent with an IV dose, blood had the highest predicted radiation exposure (0.01308 rem). The maximum predicted whole body exposure to radioactivity from a 100 µCi, IV dose of [¹⁴C]VNP40101M to humans was estimated to be 0.0566 rem, which was approximately 1.9% of the 3 rem limit specified by the Code of Federal Regulations (21 CFR: part 361.1, section b, 3i). The cumulated exposure, estimated using the proposed human dose and longest tissue half-life for the rat, was 37728 µCi·h.

Metabolite/decomposition products of laromustine formed *in vitro* and *in vivo*

Table 4 shows the structures, molecular formula and the molecular weights of the metabolite/decomposition products of laromustine formed in HLM incubations and rat plasma *in vivo*. Detailed results from experiments with radioactive ¹⁴C-laromustine, cross-species liver microsomes, *in vitro* mass balance and reaction phenotyping are reported elsewhere (Nassar et al., 2009).

Conclusions

This study is the first QWBA to provide images of whole-body biodistribution of radiolabeled laromustine. Drug-derived radioactivity was widely distributed to tissues through 7 days post-dose after a single 10 mg/kg IV bolus dose of [¹⁴C]VNP40101M to male pigmented rats. Maximum concentrations were observed at 0.5 or 1 h post-dose for majority of tissues (28 of 42). The highest concentrations of radioactivity were found in the small intestine contents at 0.5 h (112.137 µg equiv/g), urinary bladder contents at 3h (89.636 µg equiv/g) and probably reflect excretion of drug and metabolites. The highest concentrations in specific organs were found in the renal cortex at 1 h (28.582 µg equiv/g), small intestine at 3h (16.946 µg equiv/g), Harderian gland at 3h (12.332 µg equiv/g) and pancreas at 3h (12.635 µg equiv/g). Concentrations in the cerebrum, cerebellum, medulla and spinal cord were maximal at 0.5 h post-dose and persisted for 7 days. Selective distribution into, or retention by, melanin containing tissues was not apparent. The predicted total body and target organ exposures for humans given a single 100 µCi IV dose of [¹⁴C]VNP40101M were well within the medical guidelines for maximum radioactivity exposures in human subjects.

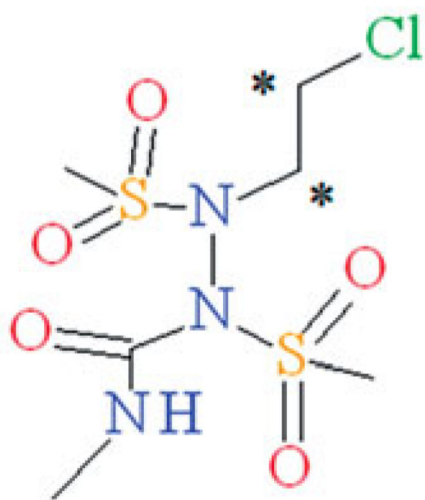
Acknowledgements

This work was done at QPS for Vion Pharmaceuticals Inc. We would like to thank Drs. Bruce Aungst and Eric Solon of QPS for supervising the studies.

References

- Baumann RP, Seow HA, Shyam K, et al. The antineoplastic efficacy of the prodrug Cloretazine is produced by the synergistic interaction of carbamoylating and alkylating products of its activation. *Oncol Res.* 2005; 15:313–325. [PubMed: 16408696]
- Finch RA, Shyam K, Penketh PG, Sartorelli AC. 1,2-Bis(methylsulfonyl)-1-(2-chloroethyl)-2-(methylamino)-carbonylhydrazine (101M): a novel sulfonyl-hydrazine prodrug with broad-spectrum antineoplastic activity. *Cancer Res.* 2001; 61:3033–3038. [PubMed: 11306484]
- Gifford AN, Espaillet MP, Gatley SJ. Biodistribution of radiolabeled ethanol in rodents. *Drug Metab Dispos.* 2008; 36:1853–1858. [PubMed: 18566042]
- Giles F, Thomas D, Garcia-Manero G, et al. A phase I and pharmacokinetic study of VNP40101M, a novel sulfonylhydrazine alkylating agent, in patients with refractory leukemia. *Clin Cancer Res.* 2004; 10:2908–2917. [PubMed: 15131024]
- Nassar, AE.; Du, J.; Lin, K., et al. Case study: the unanticipated loss of N2 from novel DNA alkylating agent Laromustine by collision-induced dissociation: novel rearrangements [Chapter 5]. Hoboken (NJ): John Wiley & Sons; 2010b.
- Nassar, AE.; Du, J.; Lin, K., et al. Case study: identification of in vitro metabolite/decomposition products of the novel DNA alkylating agent laromustine [Chapter 6]. Hoboken (NJ): John Wiley & Sons; 2010c.
- Nassar AE, King I, Paris BL, et al. An in vitro evaluation of the victim and perpetrator potential of the anti-cancer agent laromustine (VNP40101M), based on reaction phenotyping and inhibition and induction of cytochrome P450 (CYP) enzymes. *Drug Metab Dispos.* 2009; 37:1922–1930. [PubMed: 19520774]
- Nassar A-EF, Du J, Belcourt M, et al. In vitro profiling and mass balance of the anti-cancer agent laromustine [¹⁴C]-VNP40101M by rat, dog, monkey and human liver microsomes. *Open Drug Metab J.* 2010a; 4:1–9.
- Nassar A-EF, King I, Du J. Characterization of short-lived electrophilic metabolites of the anticancer agent laromustine (VNP40101M). *Chem Res Toxicol.* 2011; 24:568–578. [PubMed: 21361357]

- Park YH, Jung BH, Chung BC, et al. Metabolic disposition of the new fluoroquinolone antibacterial agent DW116 in rats. *Drug Metab Dispos.* 1997; 25:1101–1103. [PubMed: 9311628]
- Penketh PG, Shyam K, Baumann RP, et al. 1,2-Bis(methylsulfonyl)-1-(2-chloroethyl)-2-[(methylamino)carbonyl] hydrazine (VNP40101M): I. Direct inhibition of O6-alkylguanine-DNA alkyltransferase (AGT) by electrophilic species generated by decomposition. *Cancer Chemother Pharmacol.* 2004; 53:279–287. [PubMed: 14704831]
- Penketh PG, Shyam K, Sartorelli AC. Comparison of DNA lesions produced by tumor inhibitory 1,2-bis(sulfonyl)-hydrazines and chloroethylnitrosoureas. *Biochem Pharmacol.* 2000; 59:283–291. [PubMed: 10609557]
- Schadt S, Kallbach S, Almeida R, Sandel J. Investigation of Figopitant and its metabolites in rat tissue by combining whole-body autoradiography with liquid extraction surface analysis mass spectrometry. *Drug Metab Dispos.* 2012; 40:419–425. [PubMed: 22184457]
- Scicinski J, Oronsky B, Taylor M, et al. Preclinical evaluation of the metabolism and disposition of RRx-001, a novel investigative anticancer agent. *Drug Metab Dispos.* 2012; 40:1810–1816. [PubMed: 22699395]
- Wang L, He K, Maxwell B, et al. Tissue distribution and elimination of [¹⁴C]apixaban in rats. *Drug Metab Dispos.* 2011; 39:256–264. [PubMed: 21071521]



VNP40101M

Asterisk indicates position of the ^{14}C -label

Figure 1.
Chemical structure of [^{14}C]laromustine (VNP40101M).

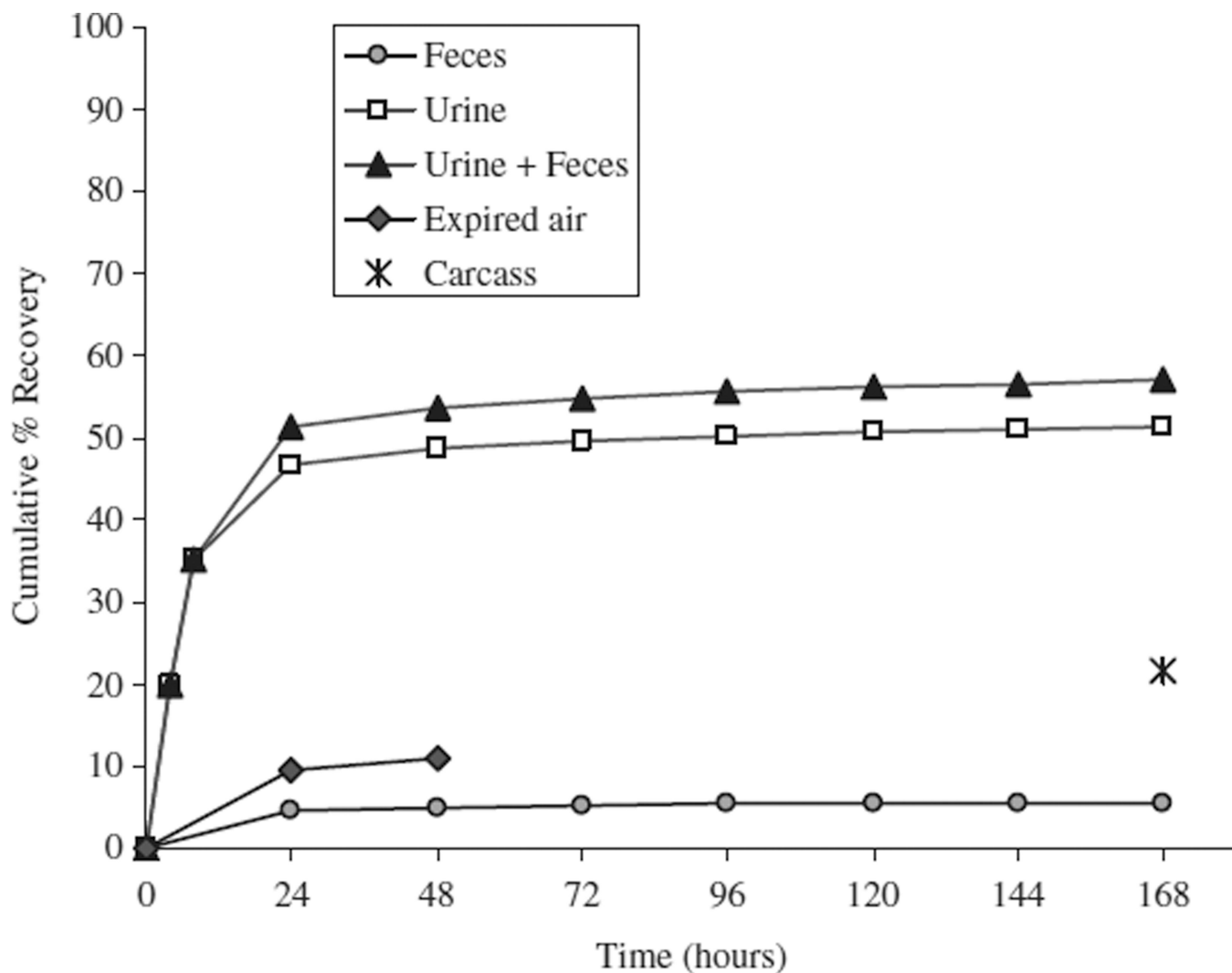


Figure 2. Mean cumulative recovery of radioactivity in urine and feces of Group 1 rats, expired air of Group 2 rats and carcasses of Group 1 rats following an intravenous bolus dose of [¹⁴C]VNP40101M at a target dose of 10 mg/kg.

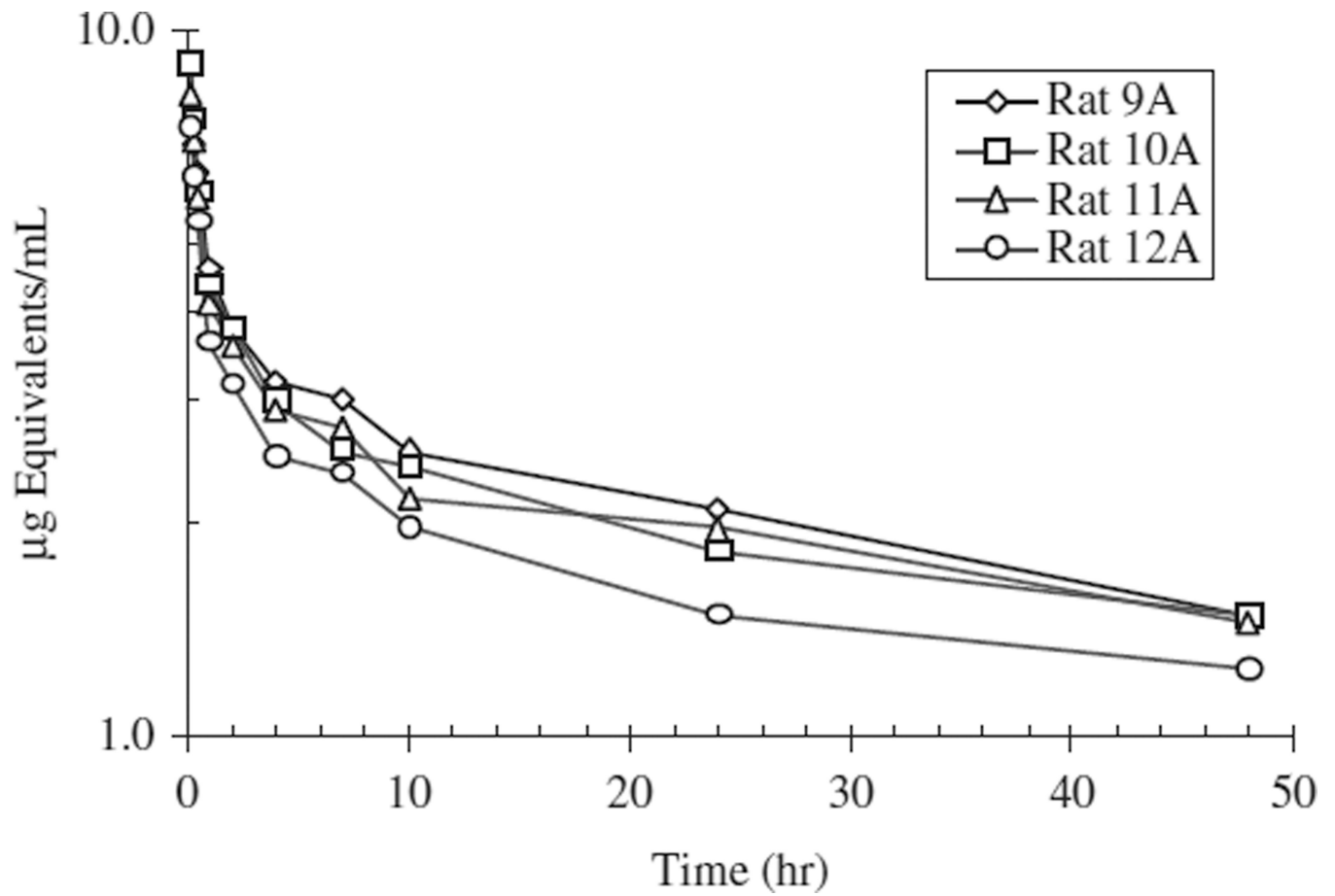


Figure 3. Individual plasma concentrations of total radioactivity versus time in Group 3 male rats following intravenous bolus target dose of 10 mg/kg.

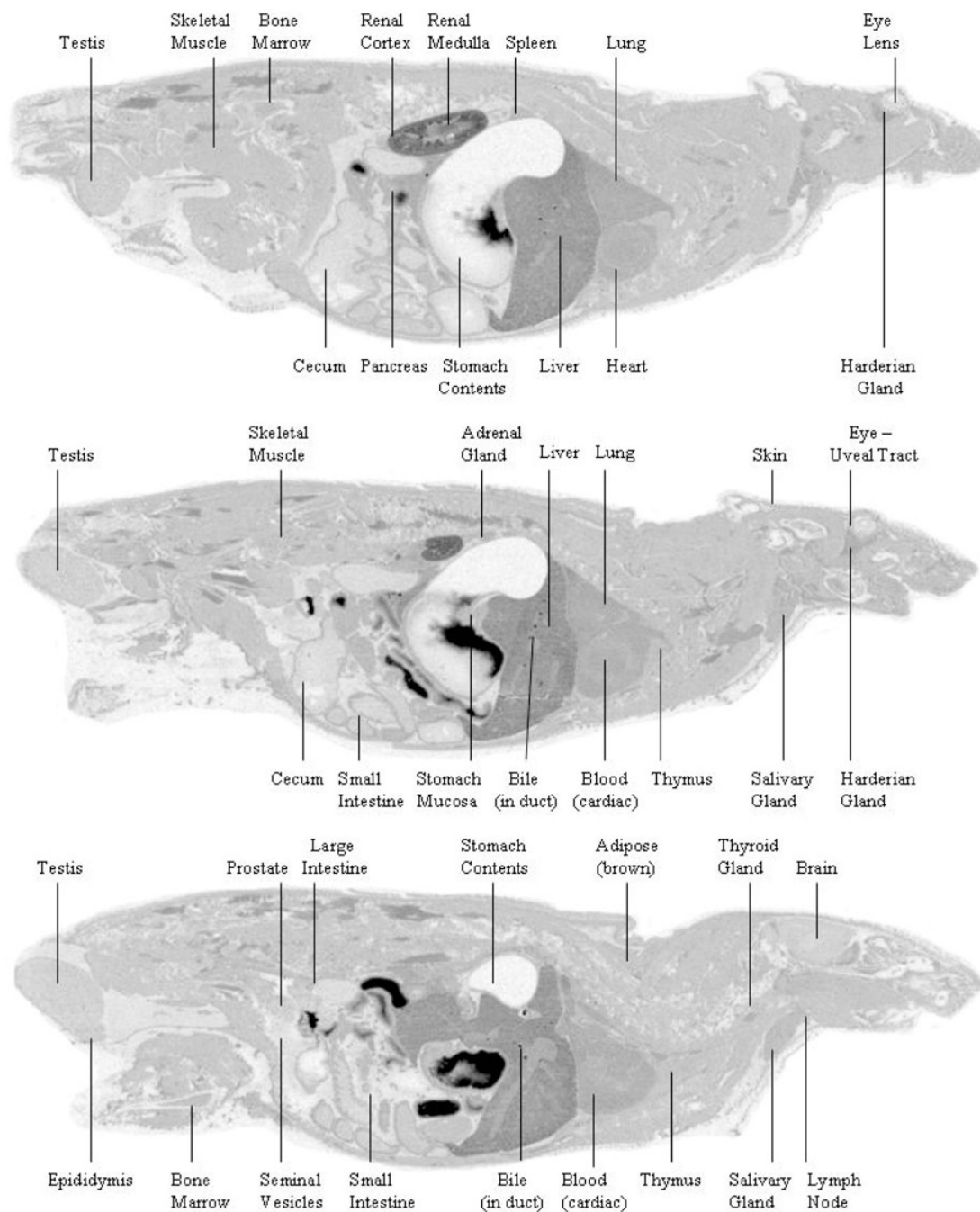


Figure 4. Whole-body autoradiogram of the radioactivity distribution in a male pigmented rat at 0.5 h post-dose (rat # 2) following a single IV administration of [¹⁴C]VNP40101M at a target dose of 10 mg/kg.

Individual and mean plasma concentrations and pharmacokinetics of total radioactivity following intravenous bolus dose administration of 10 mg/kg [¹⁴C]VNP40101M to Group 3 rats.

Table 1

Time	Plasma μg Equivalents/mL					
	Rat 9A	Rat 10A	Rat 11A	Rat 12A	Mean	SD
0	BQL	BQL	BQL	BQL	0.000	0.000
0.083	8.973	9.000	8.126	7.310	8.352	0.805
0.25	6.935	7.479	6.999	6.169	6.896	0.542
0.5	6.297	5.855	5.837	5.366	5.839	0.380
1	4.599	4.358	4.084	3.614	4.164	0.423
2	3.766	3.758	3.561	3.136	3.555	0.295
4	3.177	2.974	2.905	2.486	2.886	0.290
7	3.013	2.536	2.721	2.357	2.657	0.280
10	2.530	2.392	2.169	1.971	2.266	0.246
24	2.093	1.831	1.969	1.490	1.846	0.260
48	1.479	1.470	1.445	1.237	1.408	0.115
C_{max} (μg equivalents/mL)	8.973	9.000	8.126	7.310	8.352	0.805
$t_{1/2}$ (min)	48.9	76.1	63.4	58.9	61.8	11.3
AUC_{0-48} ($\text{h}^*\mu\text{g/mL}$)	110.029	104.829	101.681	84.820	100.340	10.904
$AUC_{0-\text{Inf}}$ ($\text{h}^*\mu\text{g/mL}$)	214.444	295.830	233.922	189.906	233.526	45.272

BQL = 0.065 μg Equivalents/mL; treated as zero for mean and SD calculations.

Table 2

Concentrations of radioactivity in tissues of male pigmented rats after a single IV dose of [¹⁴C]VNP40101M at 10 mg/kg.

Tissue type	Tissue	µg Equivalents/g Tissue										
		0.5 h	1 h	3 h	6 h	8 h	24 h	2 d	3 d	4 d	5 d	7 d
Vascular/Lymphatic	Blood	5.612	5.927	5.983	4.987	5.380	3.675	3.286	3.380	2.081	2.565	1.834
	Bone marrow	3.834	4.589	3.174	2.548	2.221	1.219	0.636	0.631	0.458	0.517	0.190
	Lymph node	5.091	3.983	4.709	1.759	1.247	1.398	0.467	0.354	0.495	0.656	0.271
Excretory/Metabolic	Spleen	4.664	5.193	4.797	2.679	2.154	1.227	1.063	0.906	0.688	0.807	0.443
	Thymus	3.336	4.044	6.848	5.338	5.253	1.901	0.838	0.465	0.435	0.285	0.214
	Bile (in duct)	17.893	34.156	5.036	4.707	4.052	1.852	2.005	2.778	0.887	0.736	0.228
	Renal cortex	18.147	28.582	15.188	3.907	3.536	1.600	1.412	0.999	0.806	0.766	0.466
	Renal medulla	10.548	8.686	4.008	4.925	5.554	1.461	1.226	0.772	0.844	0.704	0.367
Central Nervous System	Liver	10.075	11.807	8.503	3.220	4.743	1.792	1.112	0.720	0.700	0.806	0.537
	Urinary bladder	4.605	4.306	4.407	1.808	0.780	4.636	0.841	1.828	0.570	1.143	0.424
	Urinary bladder (contents)	43.156	49.231	89.636	0.628	0.496	2.221	0.843	0.310	0.218	0.179	0.143
	Brain (cerebrum)	1.978	1.359	1.026	0.574	0.887	0.397	0.290	0.197	0.135	0.178	0.157
	Brain (cerebellum)	2.109	1.273	0.985	0.763	1.027	0.634	0.404	0.269	0.211	0.234	0.175
Endocrine	Brain (medulla)	1.797	1.126	0.745	0.622	0.804	0.412	0.303	0.214	0.110	0.162	0.145
	Spinal cord	1.510	1.174	0.871	0.567	0.572	0.345	0.194	0.262	0.129	0.168	0.133
	Adrenal gland	4.772	3.949	3.980	2.100	2.230	1.416	1.110	0.830	0.841	0.799	0.592
	Pituitary gland	4.289	4.107	5.612	2.132	2.003	0.734	0.488	0.500	0.305	0.349	NS
Secretory	Thyroid	5.795	5.931	3.003	1.709	1.641	0.865	0.629	0.531	0.316	0.508	0.246
	Harderian gland	5.755	10.686	12.332	3.668	2.529	1.342	0.918	0.671	0.497	0.368	0.182
Adipose	Pancreas	6.423	9.069	12.635	6.913	5.459	1.949	0.703	0.591	0.369	0.372	0.247
	Salivary gland	4.432	4.219	3.690	2.393	2.383	0.911	0.662	0.467	0.371	0.346	0.225
	Adipose (brown)	3.776	4.599	2.642	1.920	2.349	1.058	0.899	0.843	0.419	0.613	0.518
Dermal	Adipose (white)	1.101	0.992	0.487	0.364	0.260	0.219	0.196	0.157	0.177	0.220	0.145
	Skin	3.785	3.345	2.910	3.259	3.191	1.093	0.766	0.465	0.875	0.475	0.195
Reproductive	Epididymis	3.205	2.272	3.561	1.486	1.295	0.452	0.416	0.358	0.210	0.237	0.168
	Prostate gland	2.350	2.037	1.764	1.451	1.133	0.703	0.688	0.431	NI	0.309	0.156
	Seminal vesicles	2.299	1.227	0.849	0.619	0.682	0.604	0.468	0.557	0.408	0.290	0.247

Tissue type	Tissue	µg Equivalents/g Tissue										
		0.5 h	1 h	3 h	6 h	8 h	24 h	2 d	3 d	4 d	5 d	7 d
	Testis	2.555	2.091	2.982	0.960	0.828	0.474	0.304	0.281	0.196	0.212	0.123
Skeletal/Muscular	Bone	0.405	0.395	0.331	0.134	0.201	BQL	BQL	BQL	0.108	BQL	BQL
	Heart	4.869	4.357	3.512	2.346	2.173	1.283	1.113	0.829	0.637	0.534	0.443
Ocular	Skeletal muscle	3.507	2.458	1.829	1.463	1.163	0.905	0.739	0.612	0.577	0.572	0.395
	Eye – Lens	BQL	0.213	0.284	0.328	0.440	0.275	0.211	BQL	BQL	BQL	BQL
Respiratory Tract	Eye – Uveal Tract	3.335	3.035	1.690	1.008	0.834	0.447	0.406	0.307	BQL	BQL	0.119
	Lung	6.124	7.151	5.397	4.288	3.516	3.103	2.232	1.999	1.526	1.729	1.145
Alimentary Canal	Cecum	3.398	4.094	3.889	2.937	3.293	0.821	0.366	0.546	0.390	0.313	0.225
	Cecum (contents)	1.267	1.290	5.900	21.516	6.161	0.364	0.119	0.133	BQL	BQL	BQL
Large intestine	Large intestine	3.364	3.237	2.444	1.577	0.960	0.887	0.515	0.377	0.290	0.230	0.298
	Large intestine (contents)	1.207	0.635	1.543	36.972	27.194	0.653	NI	0.110	BQL	BQL	BQL
Stomach (gastric mucosa)	Stomach (gastric mucosa)	3.866	4.872	4.059	2.639	1.480	0.748	0.370	0.578	0.228	0.393	0.203
	Stomach (contents)	8.580	6.386	0.126	0.199	0.310	0.120	BQL	BQL	BQL	BQL	BQL
Small intestine	Small intestine	4.231	8.295	16.946	2.793	1.921	1.015	0.454	0.300	0.281	0.223	0.219
	Small intestine (contents)	112.137	67.725	7.717	1.507	0.627	0.933	0.186	BQL	0.122	0.143	BQL

NI, Not identified during tissue collection; NS, Not sampled, since not visualized on autoradioluminograph, considered as BQL; BQL, Value is below the LLOQ.

LLOQ = 0.0008426 µCi/g/0.007829 µCi/µg = 0.108 µg equivalent/g tissue.

ULOQ = 8.177 µCi/g/0.007829 µCi/µg = 1044.450 µg equivalent/g tissue.

Table 3

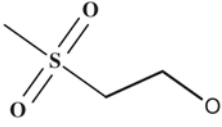
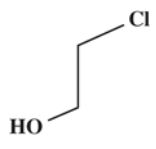
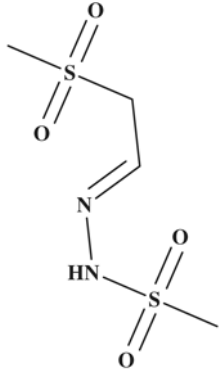
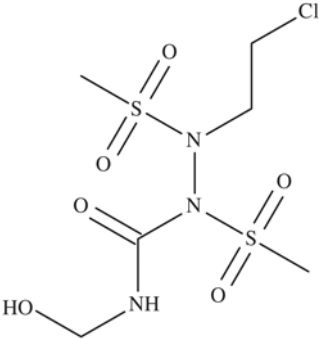
Predicted tissue exposure in humans given a single 100 μ Ci IV dose of [14 C] VNP40101M.

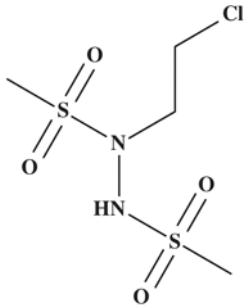
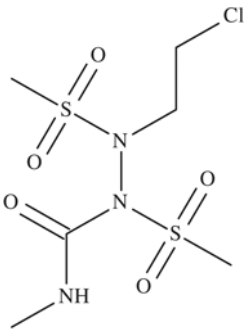
Organ system	Organ/Tissue	C_{max} (μ Ci/g)	T_{max} (h)	r^2	# of pts for $t_{1/2}$	$t_{1/2}$ (h)	AUCinf (obs) (μ Ci-h/g)	D Rat (rem)	D Human (rem)	D Human (mrem)
Adipose	Adipose (brown)	0.0360	1.00	0.99	4	147	2.032	0.213	0.00389	3.8882
	Adipose (white)	0.0086	0.50	0.96	3	262	0.688	0.072	0.00132	1.3159
Alimentary Canal	Cecum	0.0320	1.00	0.99	5	76	1.132	0.119	0.00217	2.1661
	Large intestine	0.0263	0.50	0.88	3	170	1.242	0.130	0.00238	2.3765
	Small intestine	0.1327	3.00	0.86	4	62	1.234	0.130	0.00236	2.3617
	Stomach	0.0381	1.00	0.95	4	79	0.978	0.103	0.00187	1.8705
Central Nervous System	Brain (cerebellum)	0.0165	0.50	0.89	4	114	0.731	0.077	0.00140	1.3989
	Brain (cerebrum)	0.0155	0.50	0.98	3	125	0.592	0.062	0.00113	1.1335
	Brain (medulla)	0.0141	0.50	0.93	4	114	0.544	0.057	0.00104	1.0409
	Spinal cord	0.0118	0.50	0.99	4	97	0.465	0.049	0.00089	0.8892
Dermal	Skin	0.0296	0.50	0.88	5	66	1.294	0.136	0.00248	2.4766
	Adrenal gland	0.0374	0.50	0.88	5	152	2.440	0.256	0.00467	4.6680
Endocrine	Pituitary gland	0.0439	3.00	0.88	4	104	1.167	0.123	0.00223	2.2329
	Thyroid	0.0464	1.00	1.00	3	87	1.143	0.120	0.00219	2.1859
Excretory/Metabolic	Liver	0.0924	1.00	0.95	3	119	2.542	0.267	0.00486	4.8643
	Renal cortex	0.2238	1.00	0.97	6	82	2.597	0.273	0.00497	4.9679
	Renal medulla	0.0826	0.50	0.92	6	79	2.086	0.219	0.00399	3.9916
	Urinary bladder	0.0363	24.00	0.89	4	81	2.374	0.249	0.00454	4.5425
Ocular	Eye Lens	0.0034	8.00	1.00	2	ND	0.267	0.028	0.00051	0.5115
	Eye Uveal tract	0.0261	0.50	0.89	5	61	0.493	0.052	0.00094	0.9434
Reproductive	Epididymis	0.0279	3.00	0.87	6	96	0.768	0.081	0.00147	1.4688
	Prostate gland	0.0184	0.50	0.96	5	65	0.724	0.076	0.00139	1.3851
	Seminal vesicles	0.0180	0.50	0.89	6	107	0.895	0.094	0.00171	1.7129
	Testis	0.0233	3.00	0.87	5	100	0.623	0.065	0.00119	1.1920
Respiratory	Lung	0.0560	1.00	0.86	5	136	4.591	0.482	0.00878	8.7836
	Harderian gland	0.0966	3.00	0.99	6	51	1.481	0.156	0.00283	2.8342
Secretory	Pancreas	0.0989	3.00	0.94	5	80	1.882	0.198	0.00360	3.6002

Organ system	Organ/Tissue	C_{max} ($\mu\text{Ci/g}$)	T_{max} (h)	r^2	# of pts for $t_{1/2}$	$t_{1/2}$ (h)	AUCinf (obs) ($\mu\text{Ci}\cdot\text{h/g}$)	D Rat (rem)	D Human (rem)	D Human (mrem)
Skeletal/Muscular	Salivary gland	0.0347	0.50	0.96	5	84	1.142	0.120	0.00219	2.1851
	Bone	0.0032	0.50	1.00	2	ND	0.141	0.015	0.00027	0.2695
	Heart	0.0381	0.50	0.96	6	90	1.717	0.180	0.00328	3.2844
Vascular/Lymphatic	Skeletal muscle	0.0275	0.50	0.93	6	135	1.544	0.162	0.00295	2.9543
	Blood	0.0468	3.00	0.92	4	138	6.836	0.718	0.01308	13.0793
	Bone marrow	0.0359	1.00	1.00	3	57	1.157	0.122	0.00221	2.2141
	Lymph node	0.0399	0.50	0.97	4	66	1.192	0.125	0.00228	2.2808
	Spleen	0.0407	1.00	0.89	6	108	1.930	0.203	0.00369	3.6933
	Thymus	0.0536	3.00	0.92	5	65	1.575	0.165	0.00301	3.0140

ND, Not determined; unable to determine this value from the data.

Table 4Metabolite/decomposition products of laromustine formed in HLM incubation and *in vivo*.

Components	Molecular formula	MW, amu	<i>In vitro</i>	<i>In vivo</i>
 2-methylsulfonylethanol	C ₃ H ₈ O ₃	124.2	Yes	ND
 2-chloroethanol	C ₂ H ₅ ClO	80.5	Yes	NT
 N-[(E)-2-methylsulfonylethylideneamino]methanesulfonamide	C ₄ H ₁₀ N ₂ O ₄ S ₂	214.3	Yes	Yes
 1-[2-chloroethyl(methylsulfonyl)amino]-3-(hydroxymethyl)-1-methylsulfonyl-urea	C ₆ H ₁₄ ClN ₃ O ₆ S ₂	323.8	Yes	Yes

Components	Molecular formula	MW, amu	<i>In vitro</i>	<i>In vivo</i>
 <p>N'-(2-chloroethyl)-N'-methyl sulfonyl-methanesulfonylhydrazide</p>	C ₄ H ₁₁ ClN ₂ O ₄ S ₂	250.7	Yes	Yes
 <p>Parent Drug (laromustine)</p>	C ₆ H ₁₄ ClN ₃ O ₅ S ₂	307.8	Yes	Yes

ND, not detected; NT, not tested.